Few numerical aspects of the Neumann-Kelvin's model with capillary in hydrodynamics

Philippe Destuynder, Caroline Fabre, Olivier Wilk

Few numerical aspects of the Neumann-Kelvin's model with capillary in hydrodynamics

Philippe Destuynder[1], Caroline Fabre[2] and Olivier Wilk[1]
[1]Department of Mathematics,
Conservatoire National des Arts et Métiers,
292, rue Saint Martin, 75003, PARIS, FRANCE
philippe.destuynder@cnam.fr and olivier.wilk@cnam.fr
[2]Laboratoire de Mathématiques CNRS-UMR 8628,
Université de Paris sud, bat. 425, 91400 Orsay, France
caroline.fabre@u-psud.fr

Abstract

A discussion and an improvement on the Neumann-Kelvin's model are suggested in this paper. This model is used in the simulation of progressive wave phenomenon. But as mentioned by several authors [CHEN 01], [YAN 00], [RIC 96], [LIH 78], this model is ill posed unless a capillary energy is introduced. The mathematical explanation is that a compactness inversion occurs if the capillary forces are omitted. Theoretical arguments and numerical simulations are used in the following which aim at giving an explanation of what happens from a mechanical point of view.

AMS Subject Classification: Primary: 74F10, 35L85, 35R35; Secondary: 76B15, 35L70, 35Q35

Key words: water waves, instabilities, wave equations, spectral theory, non-linear models

1 Introduction

Let us consider a bounded connected and non empty open set in $\mathbb{R}^3$ denoted by Ω the boundary of which is $\partial\Omega$. This set is a water pool with a bottom Γ_0, a free surface Γ_f and two sides Γ_{1i} and Γ_{10} through which a water flow is respectively entering and leaving the pool (see figure 1). The unit normal along the boundary outwards Ω is ν. A submarine can be included in the pool and its boundary is Γ_b. Another possibility is to have a pebble stone bottom. A steady flow is entering Ω through Γ_{1i} at the normal velocity U and getting out

through Γ_{10}. There are two kinds of boundary conditions on Γ_1 depending if one considers the steady flow or the transient one. Concerning the steady flow the most realistic condition consists in fixing the normal velocity. But in the transient analysis, one can consider that the acoustic pressure in the wake is not perturbed. Nevertheless, the mathematical analysis is similar in each case. A comparaison in the numerical tests shows that the changes of boundary condition on the transient analysis are not meaningfull as far as the time delay of the simulation is small enough in order to avoid any return of surface waves. Another strategy is to use non-reflecting boundary conditions on Γ_1. But this last possibility is a little bit complex because there are several kinds of waves on the surface and the water itself is assumed to be incompressible. Therefore, this point is not discussed in this paper. Because the fluid is assumed to be unviscid, it is assumed that the flow velocity can be modelled by a potential function Φ. From the incompressibility, one can ensure that $-\Delta\Phi = 0$ in Ω. Let us denote by η the normal displacement of a geometrical point on the free surface of the water Γ_f.

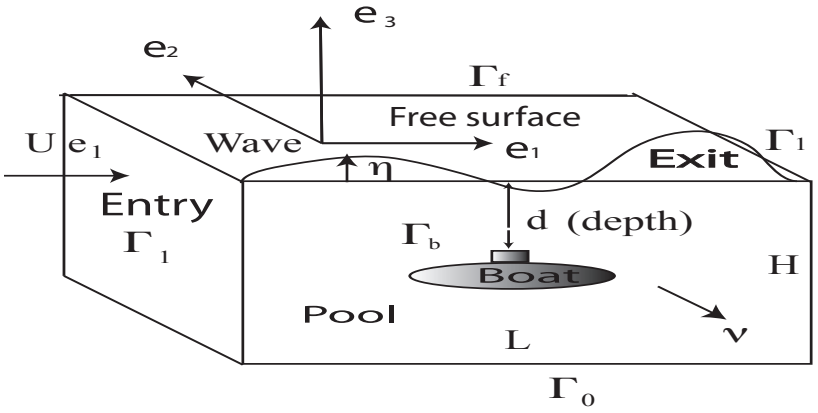

Figure 1: *Main geometrical notations*

We assume that the boundary conditions outside Γ_1 are

$$\begin{cases} \dfrac{\partial \Phi}{\partial \nu} = 0 \text{ on } \Gamma_b \cup \Gamma_0, \\ \\ \dfrac{\partial \Phi}{\partial \nu} = \dfrac{\partial \eta}{\partial t} + \nabla_s \Phi . \nabla_s \eta, \text{ on } \Gamma_f, \end{cases} \tag{1}$$

The boundary conditions on Γ_1 are defined separately in the following for the steady component and the transient one.

The stationary potential -say Φ_0- is solution of the following set of equations:

$$\begin{cases} -\Delta \Phi_0 = 0, \\ \\ \dfrac{\partial \Phi_0}{\partial \nu} = U(e_1, \nu) \text{ on } \Gamma_1, \\ \\ \dfrac{\partial \Phi_0}{\partial \nu} = 0 \text{ on } \Gamma_b \cup \Gamma_0, \\ \\ \dfrac{\partial \Phi_0}{\partial \nu} = 0 \text{ on } \Gamma_f. \end{cases} \tag{2}$$

Because Φ_0 is harmonic in Ω it is necessary that the Fredholm 's condition should be satisfied:

$$\int_{\partial\Omega} \frac{\partial \Phi_0}{\partial \nu} = 0. \tag{3}$$

In the present analysis, this relation is in fact a condition on the geometry of the boundary Γ_1 which traduces the incompressibility of the fluid. It can be explicited as follows and it is easy to ensure that it is satisfied:

$$\int_{\Gamma_1} (e_1, \nu) = 0. \tag{4}$$

In most classical analysis of progressive waves, the fonction Φ_0 is estimated by $x_1 U$ which is the right solution for a parallelepipede. Let us notice that this is not correct for instance as soon as a submarine or a pebble stone bottom is considered inside Ω. These cases are those studied in the following. The solution method used in this paper for computing Φ_0 is a finite element one. But this step could also solved by a boundary integral method
The Fredholm's condition (3) is not necessary for the transient state, as far as a Dirichlet boundary condition is prescribed on Γ_1. One practical advantage is that it avoids to add an additional constraint on η. But this could be mathematically possible without new difficulties excepted in the notations. In order to split the steady state and the transient state let us set:

$$\Phi = \Phi_0 + \varphi, \tag{5}$$

where Φ_0 is the solution of (2). Because Φ_0 is proportional to the boat velocity, one sets:

$$\Phi_0 = U\tilde{\Phi}_0, \tag{6}$$

where $\tilde{\Phi}_0$ is the solution of (2) with $U = 1$. The transient term φ should be solution of:

$$\begin{cases} -\Delta\varphi = 0 \text{ in } \Omega, \\ \\ \varphi = 0 \text{ on } \Gamma_1, \\ \\ \dfrac{\partial\varphi}{\partial\nu} = 0 \text{ on } \Gamma_0 \cup \Gamma_b, \\ \\ \dfrac{\partial\varphi}{\partial\nu} = \dfrac{\partial\eta}{\partial t} + U\nabla_s\tilde{\Phi}_0.\nabla_s\eta + \nabla_s\varphi.\nabla_s\eta \text{ on } \Gamma_f. \end{cases} \tag{7}$$

The last boundary condition is a non-linear one because of the term $\nabla_s\varphi.\nabla_s\eta$ and it is omitted in the linear approximation. It will be discussed later on how to take into account non-linear terms when an instability occurs in the linear model and therefore the linearization wouldn't be justified.

Several possibilities occur for the boundary condition satisfied by φ on Γ_1. The one used in (7) traduces a vanishing acoustic pressure. Another possibility would be to prescribe that the total pressure (linearized expression) is zero (assuming also that the steady velocity is normal to Γ_1):

$$\frac{\partial\varphi}{\partial t} + U\frac{\partial\varphi}{\partial\nu} = 0. \tag{8}$$

Clearly there are many other possibilities in the definition of the boundary condition that should be satisfied by φ on this part of the boundary $\partial\Omega$.

Furthermore it is certainly more realistic to use different boundary conditions at the flow-intake and the exit even if the mathematical analysis is similar. But their influence is restricted as far as the time delay for the computation doesn't allow the waves to reach the boundary of the open set Γ_f.

1.1 The equilibrium of the free surface

Let us denote by p the pressure in the fluid. From Bernoulli theorem (see for instance G. Duvaut [DUV 90] or L. Landau-E. Lipschitz [LAL 71]), one obtains on the free surface of the water -say Γ_f ($x_3 = 0$)- by considering only the linearized expression in η and φ of the pressure (p_0 is the pressure in the air over the free surface):

$$p = p_0 - \varrho\frac{\partial\varphi}{\partial t} - \frac{\varrho}{2}|\nabla\varphi|^2 - \varrho U\nabla_s\tilde{\Phi}_0.\nabla_s\varphi - \varrho\frac{U^2}{2}|\nabla_s\tilde{\Phi}_0|^2 - \varrho g\eta + \sigma\Delta_s\eta. \tag{9}$$

In this expression σ is the capillary constant, g is the gravity and ϱ is the mass density of the fluid. The notation Δ_s is the Laplace operator restricted to the free surface.

Remark 1. *One could consider a more complete expression for the capillary forces (the energy of which is proportional to the variation of surface) which is given by:*

$$div_s(\frac{\nabla_s \eta}{\sqrt{1+|\nabla_s \eta|^2}}).$$

But on the one hand the first additional non-linear term is a third order one, and on the other hand, this would lead us to use the space BV which allows discontinuities and which is much more complicated in the approximation method (see G. Aubert and P. Kornprobst [Aub 02]).

One can linearize the formula (9) by cancelling the term $|\nabla\varphi|^2$ or by linearizing it around a value φ_0 for instance corresponding to a stationary (time independent) flow different from the one induced by Φ_0. A digging effect of the free surface due to the term $-\varrho\frac{U^2}{2}|\nabla_s\tilde{\Phi}_0|^2$ can also appear in this stationary flow and it is denoted by η_0. This so-called digging component is solution of:

$$\left\{\begin{array}{l} \eta_0 \in H_0^1(\Gamma_f), \\ \\ -\sigma\Delta_s\eta_0 + \varrho g\eta_0 + \varrho U^2 \nabla_s\tilde{\Phi}_0.\nabla_s G(\nabla_s\tilde{\Phi}_0.\nabla_s\eta_0) = -\frac{\varrho U^2}{2}|\nabla_s\tilde{\Phi}_0|^2, \end{array}\right. \tag{10}$$

where $G(f) = \varphi|_{\Gamma_f}$ is the restriction on Γ_f of the solution φ of the model (7) where the boundary condition on Γ_f is replaced by $\dfrac{\partial\varphi}{\partial\nu} = f$. This operator G plays an important role in the following. For example, if $\tilde{\Phi}_0 = x_1$ and if one restricts the preceding model to a one dimensional case, one obtains the following model for the digging effect:

$$\left\{ -\sigma\Delta_s\eta_0 + \varrho g\eta_0 + \varrho U^2 \frac{\partial G(\frac{\partial\eta_0}{\partial x_1})}{\partial x_1} = -\frac{\varrho U^2}{2}. \right. \tag{11}$$

In general, the expression of the digging effect depends on the steady flow which is described by Φ_0. For instance it could be much more meaningful for shallow water and with different boundary condition on Γ_1. For sake of simplicity in the writing, let us consider here that both η_0 and φ_0 can be neglected. Therefore the linearized pressure is given by:

$$p = p_0 - \varrho\frac{\partial\varphi}{\partial t} - \varrho U\nabla_s\tilde{\Phi}_0.\nabla_s\varphi - \varrho\frac{U^2}{2}|\nabla_s\tilde{\Phi}_0|^2 - \varrho g\eta + \sigma\Delta_s\eta. \tag{12}$$

Let us adopt for instance homogeneous Dirichlet boundary conditions for η on $\partial\Gamma_f$. The equilibrium of the free surface is therefore explicited by (p_0 which acts on both side of Γ_f is eliminated):

$$-\sigma\Delta_s\eta + \varrho g\eta + \varrho\frac{\partial\varphi}{\partial t} + \varrho U\nabla_s\tilde{\Phi}_0.\nabla_s\varphi + \varrho\frac{U^2}{2}|\nabla_s\tilde{\Phi}_0|^2 = 0. \tag{13}$$

2 Formulation of the model in η

Let us introduce the functional space in which η is looked for:

$$V = H_0^1(\Gamma_f). \tag{14}$$

By multiplying equation (13) by an arbitrary element of the space V, one obtains:

$$\begin{aligned} &\forall v \in V, \\ &\sigma\int_{\Gamma_f}\nabla_s\eta.\nabla_s v + \varrho g\int_{\Gamma_f}\eta v + \varrho\int_{\Gamma_f}\frac{\partial\varphi}{\partial t}v + \varrho U\int_{\Gamma_f}\nabla_s\tilde{\Phi}_0.\nabla_s\varphi v \\ &\qquad = -\frac{\varrho U^2}{2}\int_{\Gamma_f}|\nabla_s\tilde{\Phi}_0|^2 v. \end{aligned} \tag{15}$$

Initial conditions should be added to this model. Let us set:

$$\eta(0) = \eta_0 \ \text{ and } \ \dot{\eta}(0) = \eta_1 \ \text{ on } \ \Gamma_f. \tag{16}$$

One convenient possibility in the analysis of this model is to eliminate the function φ from equation (7). In fact, as far as the non-linear term $\nabla_s\varphi.\nabla_s\eta$ is omitted in (7), φ depends linearly on η and for eliminating φ, one can introduce the following operator denoted by G which is the so-called added mass operator. Let g be an arbitrary function defined on the boundary Γ_f. The element $G(g)$ is the restriction to Γ_f of the solution to the following model:

$$\begin{cases} -\Delta\Phi = 0 \text{ in } \Omega, \\ \dfrac{\partial\Phi}{\partial\nu} = 0 \text{ on } \Gamma_0\cup\Gamma_b, \\ \Phi = 0 \text{ on } \Gamma_1, \\ \dfrac{\partial\Phi}{\partial\nu} = g \text{ on } \Gamma_f. \end{cases} \tag{17}$$

It is proved in [DCF 09] that G^{-1} is an isomorphisme between the spaces $\tilde{H}^{1/2}(\Gamma_f)$ and its dual. Definitions and details on these fractional spaces can

be found in R. Adams [ADA 75] or J.L. Lions and E. Magenes [LM 68]. In our case, the elements of $\tilde{H}^{1/2}(\Gamma_f)$ are defined as the restriction to Γ_f of functions lying in $H^1(\Omega)$ and which are zero on Γ_1. Let us just point out for our purpose that the natural embedding from $\tilde{H}^{1/2}(\Gamma_f)$ into $L^2(\Gamma_f)$ is compact as the one from $L^2(\Gamma_f)$ into $[\tilde{H}^{1/2}(\Gamma_f)]'$ which is the dual space of $\tilde{H}^{1/2}(\Gamma_f)$. The norm on $\tilde{H}^{1/2}(\Gamma_f)$ is denoted by $|||\ |||_{1/2}$ and the one of its dual space is $|||\ |||_{-1/2}$. The former is defined by:

$$|||g|||_{1/2} = \inf_{\substack{v = g \text{ on } \Gamma_f \\ v = 0 \text{ on } \Gamma_f}} ||v||_{1,\Omega}.$$

From the linearity of G one can write (let us recall that the non-linear term $\nabla_s\varphi.\nabla_s\eta$ is omitted):

$$\varphi_{|\Gamma_f} = G(\frac{\partial \eta}{\partial t}) + UG(\nabla_s\eta.\nabla_s\tilde{\Phi}_0). \tag{18}$$

By introducing this expression into the equation (13) which traduces the equilibrium of the free surface, one obtains formally (an integration by parts has been used and boundary terms have disappeared because $v = 0$ on $\partial\Gamma_f$):

$$\begin{cases} \forall t \in [0,T],\ \eta(t) \in H_0^1(\Gamma_f), \\ \\ \forall v \in H_0^1(\Gamma_f),\ m_s(\dfrac{\partial^2 \eta}{\partial t^2}, v) + 2Uc(\dfrac{\partial \eta}{\partial t}, v) + a(\eta, v) = 0, \\ \\ \eta(0) = \eta_0,\ \ \dfrac{\partial \eta}{\partial t}(0) = \eta_1 \text{ on } \Gamma_f. \end{cases} \tag{19}$$

with the notations:

$$\begin{cases} \forall \eta, v \text{ smooth enough :} \\ \\ m_s(\eta, v) = \varrho \displaystyle\int_{\Gamma_f} G(\eta)v, \\ \\ c(\eta, v) = \dfrac{\varrho}{2} \displaystyle\int_{\Gamma_f} \big[G(\nabla_s\tilde{\Phi}_0.\nabla_s\eta)v - \nabla_s\tilde{\Phi}_0.\nabla_s v\ G(\eta) - \Delta_s\tilde{\Phi}_0 G(\eta)v\big], \\ \\ a(\eta, v) = \displaystyle\int_{\Gamma_f} \big[\sigma\nabla_s\eta.\nabla_s v + \varrho g\eta v\big] \\ \\ -\varrho U^2 \displaystyle\int_{\Gamma_f} \big[G(\nabla_s\tilde{\Phi}_0.\nabla_s\eta)\nabla_s\tilde{\Phi}_0.\nabla_s v + \Delta_s\tilde{\Phi}_0 G(\nabla_s\tilde{\Phi}_0.\nabla_s\eta)v\big]. \end{cases} \tag{20}$$

In many examples the effect of the term $\Delta_s\tilde{\Phi}_0$ is numerically neglectible as far as they are no surface ship. This point is observed in the numerical tests, even

if it is not zero. First of all let us check few useful properties of the bilinear forms m_s, c and a. Let us notice that they are well defined if η and v are functions lying in the space $H_0^1(\Gamma_f)$. It is also worth noting that the classical symmetry property holds for G:

$$\forall \eta, v \in L^2(\Gamma_f),\ \int_\Omega \nabla\Phi(\eta).\nabla\Phi(v) = \int_{\Gamma_f} G(\eta)\Phi(v) = \int_{\Gamma_f} G(v)\Phi(\eta), \qquad (21)$$

which implies the symmetry of the bilinear form m_s. This is also true for the three first terms in the definition of a. One can also claim that the bilinear form c restricted to its two first terms is anti-symmetrical. This is due to fact that it represents a gyroscopic coupling. In fact, $\nabla_s\eta$ is a rotation of the unit normal ν to the free surface Γ_f. But the main properties are the coerciveness properties which are summarized here-after. In order to make sense to the expressions which appear in the definitions of the bilinear forms one assumes that $\tilde{\Phi}_0 \in \mathcal{C}^3(\Gamma_f)$, (see P. Grisvard [GRI 86] or M. Borsuk and V. Kondratiev [KON 06] for the justification) because one has in this case:

$$\left\{ \begin{array}{l} |\displaystyle\int_{\Gamma_f} \Delta_s\tilde{\Phi}_0 G(\eta)v| \le c|||\eta|||_{-1/2,\Gamma_f}\ \ |||v|||_{-1/2,\Gamma_f}, \\ \\ \text{and:} \\ \\ |\displaystyle\int_{\Gamma_f} -\Delta_s\tilde{\Phi}_0 G(\nabla_s\tilde{\Phi}_0.\nabla_s\eta)v| \le c|||v|||_{1/2,\Gamma_f}\ \ ||\nabla_s\tilde{\Phi}_0.\nabla_s\eta||_{-1/2,\Gamma_f} \\ \\ \qquad\qquad \le c'||\eta||_{1/2,\Gamma_f}\ \ |||v|||_{1/2,\Gamma_f} \end{array} \right. \qquad (22)$$

Let us mention a result [DCF 09] which enables to justify the model used.

Theorem 1. *Let us assume that* $\min(\varrho g, \sigma) > 0$. *Then, there exists constants* $c_i > 0$ *and a scalar* $\lambda_1 > 0$ *such that:*

$$\left| \begin{array}{l} \forall \eta, v \in H_0^1(\Gamma_f) : \\ \\ \quad a(v,v) \ge c_0||v||^2_{1,\Gamma_f} - c_5U^2||v||^2_{1/2,\Gamma_f} \ge c_6(\lambda_1 - U^2)||v||^2_{1,\Gamma_f}, \\ \\ m_s(v,v) \ge c_1|||v|||^2_{-1/2,\Gamma_f}, \\ \\ |m_s(\eta,v)| \le c_2|||\eta|||_{-1/2,\Gamma_f}\ |||v|||_{-1/2,\Gamma_f},\ \ |a(\eta,v)| \le c_3||\eta||_{1,\Gamma_f}\ ||v||_{1,\Gamma_f}, \\ \\ |c(\eta,v)| \le c_4||\eta||_{1/2,\Gamma_f}\ ||v||_{1/2,\Gamma_f}. \end{array} \right.$$

The main application concerns the existence and uniqueness of a solution to the coupled model (19) for any velocity U and for ad hoc initial conditions η_0 and η_1.

Remark 2. *A natural question is to obtain the best constant λ_1 which appears in the previous theorem. This is discussed in the following. It leads to the first critical velocity which would be equal to $\sqrt{\lambda_1}$.*

Remark 3. *One can consider several kind of boundary conditions on $\partial\Gamma_f$ concerning η. For instance, one can set:*

$$\frac{\partial \eta}{\partial \nu} + \alpha\eta = 0 \text{ sur } \partial\Gamma_f, \tag{23}$$

which is a Robin's boundary condition. If $\alpha = 0$ there is a perfect gliding of the water, if $\alpha = \infty$ there is an adhesion of the water which is the case considered here. But the influence on the results is not important as far as the time is small enough in order to avoid rebounds of waves on the boundary $\partial\Gamma_f$. One can also consider a condition as:

$$\frac{\partial \eta}{\partial t} + \gamma\frac{\partial \eta}{\partial \nu} + \delta\eta = 0, \tag{24}$$

and so on. The most suitable boundary condition for η is certainly a transparency one in order to avoid reflection. But it would also be useful to use such a condition for φ on Γ_1.

2.1 About the static instabilities

The existence (and uniqueness) theorem of a solution in η is true for any U. But the stability requires the hypothesis: $U < \sqrt{\lambda_1}$ where λ_1 is a constant which appears in the coerciveness on the space $H_0^1(\Gamma_f)$ of $a(.,.)$ (see theorem 1). Let us discuss the best value for the constant λ_1 in the particular case where the term $\Delta_s\tilde{\Phi}_0$ is zero (neglected). In this case, the bilinear form a is symmetrical and c is antisymmetrical. Two cases have to be considered depending if there is a capillary term or not ($\sigma > 0$ and $\sigma = 0$).

Let us introduce the eigenvalue model:

$$\left\{\begin{array}{l} \text{find } (\lambda, w) \in \mathbb{R}^+ \times H_0^1(\Gamma_f) \text{ such that:} \\ \\ \forall v \in H_0^1(\Gamma_f) : \\ \\ \lambda\varrho \displaystyle\int_{\Gamma_f} G(\nabla_s\tilde{\Phi}_0.\nabla_s w)\nabla_s\tilde{\Phi}_0.\nabla_s v = \sigma \int_{\Gamma_f} \nabla_s w.\nabla_s v + \varrho g \int_{\Gamma_f} wv, \\ \\ \varrho \displaystyle\int_{\Gamma_f} G(\nabla_s\tilde{\Phi}_0.\nabla_s w)\nabla_s\tilde{\Phi}_0.\nabla_s w = \varrho \int_{\Omega} |\nabla\Phi(\nabla_s\tilde{\Phi}_0.\nabla_s w)|^2 = 1. \end{array}\right. \tag{25}$$

The non-trivial solutions of:

$$v \in H_0^1(\Gamma_f),\ \nabla_s\tilde{\Phi}_0.\nabla_s\eta = 0,$$

play a particular role in the stability analysis. For instance in one dimension, one can prove (see [DCF 09] that the only solution is zero. But this result is true in many cases excepted may be for very particular geometries of the surface Γ_f. From general spectral theory of linear operators one can deduce the following theorem:

Theorem 2. *Let us assume for sake of simplicity that the set:*

$$K_0 = \{v \in H_0^1(\Gamma_f),\ \nabla_s\tilde{\Phi}_0.\nabla_s v = 0\},$$

is reduced to $\{0\}$. *Two cases are considered in which the results are inverted.*
1 • If $\sigma > 0$, *there exists a countable set of elements denoted by* (λ_n, w_n) *in* $\mathbb{R}^{+*} \times H_0^1(\Gamma_f)$ *solution of (25). Each term of the sequence (ordered by increasing values)* λ_n *has a finite multiplicity (*∞ *is the only accumulation point). The family* $\{\frac{w_n}{\sqrt{\lambda_n}}\}$ *is an Hilbert basis of the space* $H_0^1(\Gamma_f)$. *The smallest eigenvalue denoted by* λ_1 *will be the best constant in theorem 1.*

2 • If $\sigma = 0$. *Let us restrict our analysis to the one dimensional case. The result is opposite to the one of the first case. There exists a countable set of solutions* $(\lambda_n, w_n) \in \mathbb{R}^{+*} \times L^2(\Gamma_f)$ *and the terms of the sequence* λ_n *are ordered by decreasing values (the largest value is denoted by* λ_1*). The multiplicity of each term is finite and* 0 *is the only accumulation point. The family* $\{w_n\}$ *is an Hilbert basis of the space* $L^2(\Gamma_f)$.

Proof. Let us begin with $\sigma > 0$. The result is a direct consequence of the spectral theory for linear operator as it is presented P.A. Raviart and J.M. Thomas [RATO 83]. In fact the bilinear form:

$$(\eta, v) \to \sigma \int_{\Gamma_f} \nabla_s\eta.\nabla_s v + \varrho g \int_{\Gamma_f} \eta v,$$

is symmetrical, continuous and coercive on the space $H_0^1(\Gamma_f)$. Furthermore the bilinear and symmetrical form:

$$(\eta, v) \to \int_{\Gamma_f} G(\nabla_s\Phi_0.\nabla_s\eta)\nabla_s\Phi_0.\nabla_s\eta,$$

is continuous on the space $H^{1/2}(\Gamma_f)$. From the properties of G^{-1} which is an isomorphism [DCF 09] between the spaces $\tilde{H}^{1/2}(\Gamma_f)$ and its dual, one obtains:

$$\begin{cases} \exists c > 0, \ \text{ such that } \ \forall \eta \in \tilde{H}^{1/2}(\Gamma_f), \\ \\ \displaystyle\int_{\Gamma_f} G(\nabla_s\Phi_0.\nabla_s\eta)\nabla_s\Phi_0.\nabla_s\eta \geq c|||\nabla_s\Phi_0.\nabla_s\eta|||^2_{-1/2,\Gamma_f}. \end{cases}$$

The continuous mapping:

$$j:\ v\in H_0^1(\Gamma_f),\ \rightarrow\ j(v)=|||\nabla_s\Phi_0.\nabla_s v|||_{-1/2,\Gamma_f}, \tag{26}$$

is a norm on the space $H_0^1(\Gamma_f)$ (hypothesis). But even if it is a norm, it is not always equivalent to the one of the space $\tilde{H}^{1/2}(\Gamma_f)$. The completed space of $H_0^1(\Gamma_f)$ equiped with the norm (26), is at least included into $[\tilde{H}^{1/2}(\Gamma_f)]'$ and contains $\tilde{H}^{1/2}(\Gamma_f)$. The natural embedding from $H_0^1(\Gamma_f)$ into $\tilde{H}^{1/2}(\Gamma_f)$ being compact, it is also compact from $H_0^1(\Gamma_f)$ into this completed space. The assumptions of the spectral theory formulated in [RATO 83] are satisfied and the result is proved if $\sigma>0$.

Let us consider the second case: $\sigma=0$ which is much more tricky. Now the bilinear and symmetrical form:

$$(\eta,v)\rightarrow \varrho g\int_{\Gamma_j}\eta v,$$

is only equivalent to the square of the norm in the space $L^2(\Gamma_f)$. It has been assumed that j defined at (26) is a norm on the space $H_0^1(\Gamma_f)$. The embedding from $\tilde{H}^{1/2}(\Gamma_f)$ into $L^2(\Gamma_f)$ being compact, the variational eigenvalue problem is inverted. This completes the proof of theorem 2 by applying the spectral theory adapted to the variational formulation [RATO 83]. □

Remark 4. *In the first case where $\sigma>0$ one can characterize the constant λ_1 which appears in theorem 1 as the smallest eigenvalue of the model (25). Therefore there are no confusion in the notation. Let us underline that λ_1 which is the smallest eigenvalue solution of (25) satisfies:*

$$\begin{aligned}&\forall v\in H_0^1(\Gamma_f),\\ &\lambda_1\varrho\int_{\Gamma_f}G(\nabla_s\Phi_0.\nabla_s v)\nabla_s\Phi_0.\nabla_s v\leq\sigma\int_{\Gamma_f}|\nabla_s v|^2+\varrho g\int_{\Gamma_f}v^2.\end{aligned} \tag{27}$$

Hence:

$$\left\{\begin{array}{l}\forall\delta\in[0,1],\ \forall v\in H_0^1(\Gamma_f),\ \ a_s(v,v)\geq\inf(\sigma,\varrho g)(1-\delta)||v||^2_{1,\Gamma_f}\\ \qquad\qquad +\varrho(\delta\lambda_1-U^2)\displaystyle\int_{\Gamma_f}G(\nabla_s\Phi_0.\nabla_s v)\nabla_s\Phi_0.\nabla_s v.\end{array}\right. \tag{28}$$

Thus λ_1 is the best constant in theorem 1 and it enables to characterize the critical velocity U_c corresponding to the instability of the linear wave model in which the term $\Delta_s\tilde{\Phi}_0$ is neglected, by:

$$U_c=\sqrt{\lambda_1}. \tag{29}$$

If $U \geq U_c$ the coerciveness of the stiffness bilinear form on the space$H_0^1(\Gamma_f)$ is lost. But it is still true for the complementary of the finite dimensional space spanned by the eigenvectors corresponding to the eigenvalues λ_n such that $U \geq \sqrt{\lambda_n}$.

Let us now assume that $\sigma = 0$. The coerciveness of a_s is no more true on the space $H_0^1(\Gamma_f)$ but only on $L^2(\Gamma_f)$ which is not contained in $H_{00}^{1/2}(\Gamma_f)$. In fact, the contrary can be true and this would be a so-called mathematical inversion of the compactness.
For any velocity $U > 0$, there exists an infinite number of instable eigenmodes. They are more and more local (the wave length is smaller and smaller). Therefore, in a numerical approximation, the more the mesh is refined, the larger is the number of instabilities. This remark which has already been formulated in a different numerical framework by Xiao-bo Chen [CHEN 02], condemns the Neuman-Kelvin's model without capillary. In fact, the variational model (19) is fully instable for $U > 0$ excepted for a finite dimensional space spanned by a finite number of eigenmodes (see theorem 2) the eigenvalues of which -say λ_n solution of (25) with $\sigma = 0$- would satisfy:

$$\lambda_n \geq U^2. \tag{30}$$

One can draw a strange conclusion: if U is small enough and if the mesh size in a numerical approximation is large enough, the Neumann-Kelvin is stable. This is really disturbing because the true model is not. One has a numerical filtering of the instabilities due to mesh size which would be too large.

The conclusion of this section is that the Neumann-Kelvin model is non physical (instable) as far as the capillary is not taken into account (excepted if $U = 0$). This result is obviously in contradiction with the usual argument that the capillary is very small and can be neglected compared to the gravity effect.

Remark 5. *The dimension of the instable space corresponds exactly to the number of eigenvalues λ_n solution of (25) and such that:*

$$\lambda_n \leq U^2.$$

3 Numerical discussion in one dimension

Our goal is mainly to give a numerical illustration of the theoretical results obtained for the progressive wave model. The accuracy of the tests must be sufficient in order to be able to claim that our conclusions are valid. This justifies that all the tests are restricted to one dimensional models. There are four steps. The first one is to compute the steady flow in order to check the influence of the depth of a submarine with respect to the free surface of the

water or the influence of a random distribution of pebble stones on the bottom of the pool. In a second step the eigenvalue problem which characterizes the static instabilities is discussed numerically. The influence of the mesh size, of the position of the submarine and of the capillary coefficient are examined. In a third step few theoretical results concerning the evolution of the spectral density are compared with the numerical results. Finally the fourth step concerns a simulation of the progressive waves on the free surface of the water.

3.1 Computation of the steady flow Φ_0

The solution method used is a finite element method. Conformal first degree polynomials have been used with a triangular mesh for Ω. The results are quite standard but the goal is to show that the velocity on the free surface is different from U because of the effect of the submarine or the pebble stone bottom. Something similar occurs for a shallow water model with irregular bottom. The coarser meshes used are represented on figure 2. The point is important because the fact that Φ_0 is different from $x_1 + c$ destroys the possibility to use an integral formulation as it is done in most of the published papers (see for instance Chalikov [CHA 07] Chen [CHEN 01] or Doutreleau [DOU 95]). The

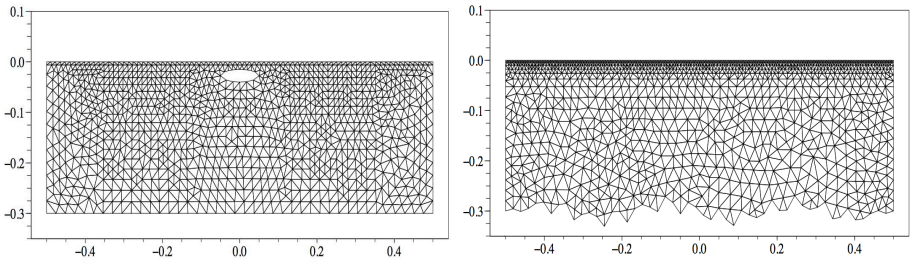

Figure 2: *The coarser meshes used for the submarine (left graph) and for the pebble stone bottom (right graph).*

isovalues of Φ_0 have been plotted for two distinct situations (a submarine and a pebble stone bottom) on figure 3 . It appears that $\nabla_s \Phi_0$ is not constant. The variations of $\nabla_s \Phi_0$ and $\Delta_s \Phi_0$ have been plotted on figure 4.

3.2 Convergence of the critical eigenvalues

The stability of the progressive wave model depends on the positiveness of the eigenvalues of the model defined at (25). Hence a numerical study is carried out in order to check the accuracy of the method which enables to compute the critical velocities U_c defined as the square root of these eigenvalues. The lowest defines the first critical velocity of the steady flow. One important feature of this mechanical phenomenon is that the spectral density is quite large and thus

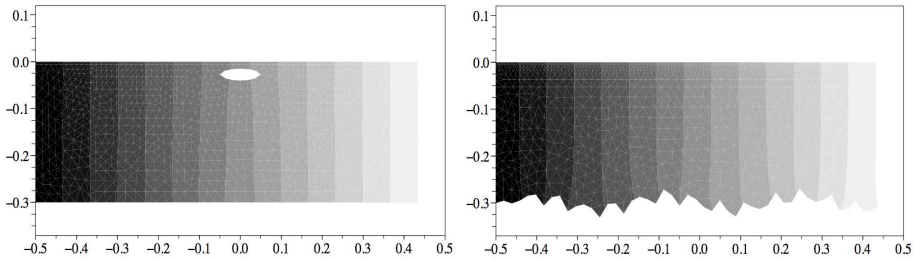

Figure 3: *The isovalues of Φ_0 are plotted for the submarine on the left and the one for the pebble stone bottom on the right.*

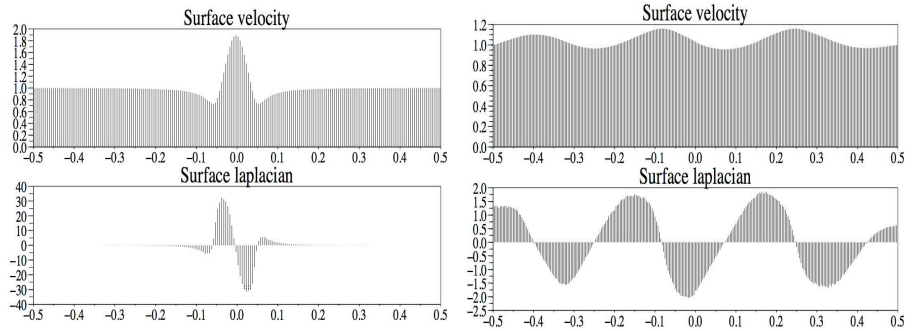

Figure 4: *On the left are the results for the submarine and on the right for the pebble stone bottom.*

the convergence is poor (see classical numerical analysis books [RATO 83]). The figure 5 shows the convergence of the eigenvalues versus mesh refinements for three different ratio between the sides of the rectangle. The computation cases correspond to a rectangular pool (without submarine). The analytical solution is known (see for instance J. Lighthill [LIH 78]).

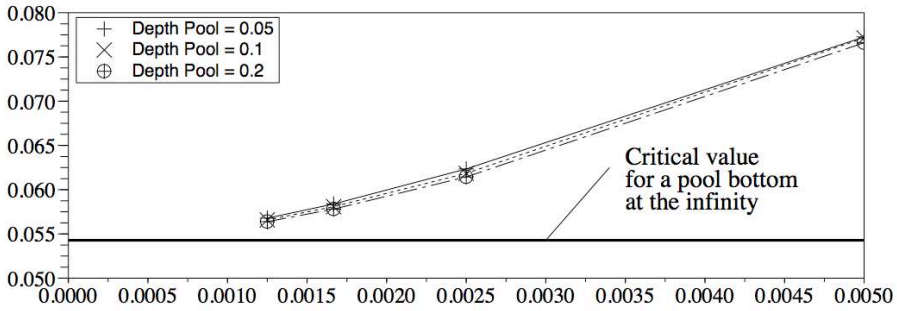

Figure 5: Convergence of the spectrum of (25) versus the mesh size for the rectangular pool without submarine (the analytical solution is known).

The figure 6 corresponds to a pebble stone bottom with three different ratio between the sides of the domain Ω. In both cases the convergence is quite slow. It is much slower than in a classical membrane model for instance and even in a Steklov's one [NEC 67]. The reason is double: first of all the compactness is only based on the compact embedding of the Sobolev's spaces $H^1(\Gamma_f)$ into $H_{00}^{1/2}(\Gamma_f)$. Secondly, the operator is not local and couples all the point of the free surface Γ_f through the operator G. For instance, if a lack of convergence appears near a corner inside of Ω it slows down the convergence everywhere and thus the eigenvalue model (25) is also degraded. The smallest eigenvalue is the square of the critical flow velocity at which a dynamic instability can occur.

3.2.1 Influence of the depth of the submarine

The computation shown in the following are performed with a refined mesh in the previous analysis. The evolution of the ten smaller eigenvalues (square of the critical velocities) have been plotted for several depths of the submarine from the free surface on figure 7. The laplacian $\Delta_s\tilde{\Phi}_0$ is kept. The smallest eigenvalue is smaller than in the analytical case used for the analysis of the convergence in the previous subsection when the submarine is quite close to the free surface and the inverse if it is quite deep. This is due to the Venturi effect between the submarine and the free surface for small depth and between the submarine and the bottom for large depth. The results obtained for $\sigma = 0$ are also drawn on figure 7. One can see that the eigenvalues are much smaller.

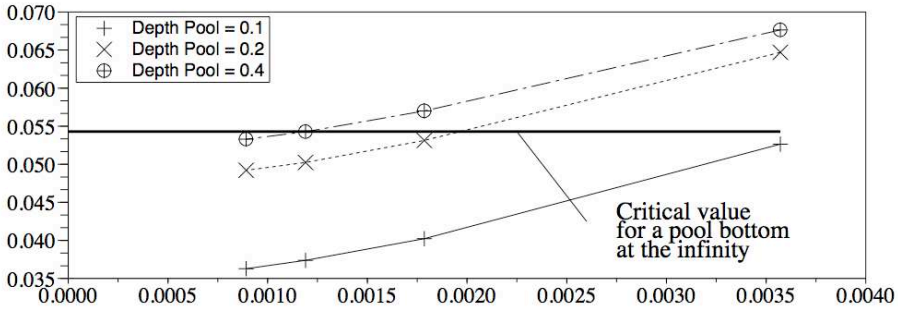

Figure 6: Convergence of the spectrum of (25) versus the mesh size for the pebble stone bottom (the analytical solution is unknown).

In a theoretical analysis of the eigen value model (25), it has been proved that for $\sigma = 0$ the sequence of the eigenvalues is upper bounded and the lower bound is zero (for the continuous model and are close to zero for a given finite element mesh). The lower graph on figure 7 shows that if the submarine is deep enough, the eigenvalues are very close from one to the other. And according to the theoretical analysis, this cluster of values tends to zero when the mesh size tends also to zero (for any depth of the submarine). At the opposite for $\sigma > 0$ the sequence of eigenvalues tends to the infinity and is lower bounded by a strictly positive number. Thus one can see that even if the capillary force are small their global energy is not. Hence it is not possible to cancel them in a realistic model for progressive waves.

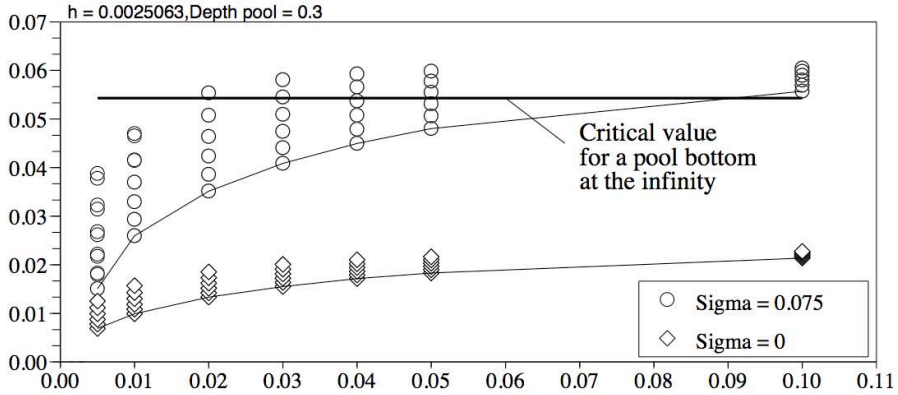

Figure 7: Influence of the depth of a submarine on the critical velocities (square) $\sigma = 7,5\ 10^{-2}$ for top curve and $\sigma = 0$ for bottom curve.

3.2.2 Influence of the depth of the pool with pebble stone bottom

The critical velocities depend on the shape of the pebble stone bottom but also on the depth of the pool. Similarly to the case of the submarine, the evolution of the spectrum has been computed and compared. The results are plotted on figure 8 depending if the capillary phenomenon is taken into account or not. Furthermore, the computation with and without the laplacian term have been compared but no meaningful influence of this term has been observed.

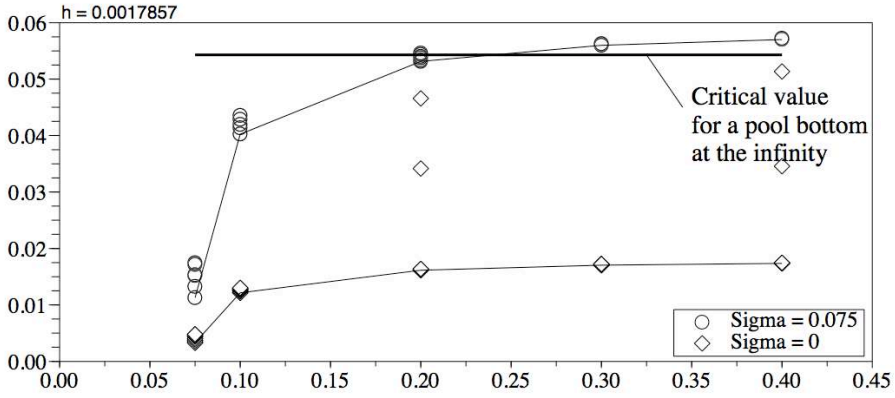

Figure 8: Influence of the depth of a pebble stone bottom pool on the critical velocities (square) $\sigma = 7.510^{-2}$ for top curve, $\sigma = 0$ for bottom curve.

3.3 About the numerical scheme used for progressive wave

Two time step schemes are discussed in this subsection but one has to be careful about the stability property. The test examples correspond to a submarine which is quite close to the free surface of the water. It is represented on the figures of section 3.4 (see figures 9 and 10).

3.3.1 A first scheme for a flow velocity such that $U < U_c$.

Let us use the progressive wave model as follows where V^h is the approximation space for the displacement η (the laplacian $\Delta_s\tilde{\Phi}_0$ is neglected for the theoretical discussion):

$$\left\{\begin{array}{l} \text{find } \eta^{n+1} \in V^h \text{ such that } \forall v \in V^h, \\ \\ m_s(\eta^{n+1} - 2\eta^n + \eta^{n-1}, v) + 2U\Delta t c_s(\eta^{n+1} - \eta^n, v) \\ \\ \qquad\qquad + \dfrac{\Delta t^2}{2} a_s(\eta^{n+1} + \eta^n, v) = F(v). \end{array}\right. \tag{31}$$

Setting $v = \eta^{n+1} - \eta^n$ in this relation, one obtains (the gyroscopic term disappears because $\mathcal{C}_s$ is antisymmetrical):

$$\begin{aligned} m_s(\frac{\eta^{n+1}-\eta^n}{\Delta t}, \frac{\eta^{n+1}-\eta^n}{\Delta t}) + \frac{1}{2}a_s(\eta^{n+1}, \eta^{n+1}) \\ = m_s(\frac{\eta^n-\eta^{n-1}}{\Delta t}, \frac{\eta^{n+1}-\eta^n}{\Delta t}) + \frac{1}{2}a_s(\eta^n, \eta^n). \end{aligned} \tag{32}$$

Finally, from the Schwarz's inequality (which is optimal) one deduces that:

$$\begin{aligned} \frac{1}{2}m_s(\frac{\eta^{n+1}-\eta^n}{\Delta t}, \frac{\eta^{n+1}-\eta^n}{\Delta t}) + \frac{1}{2}a_s(\eta^{n+1}, \eta^{n+1}) \\ \leq \frac{1}{2}m_s(\frac{\eta^n-\eta^{n-1}}{\Delta t}, \frac{\eta^n-\eta^{n-1}}{\Delta t}) + \frac{1}{2}a_s(\eta^n, \eta^n). \end{aligned} \tag{33}$$

This inequality ensures the stability of the scheme as soon as $U < U_c$ because the terms above represent the energy of the system. But if $U \geq U_c$ the bilinear form a_s is no more positive. Let use an Hilbert basis of the space $H_0^1(\Gamma_f)$ solution of the eigenvalue problem:

$$\left\{ \begin{array}{l} \text{find } w, \lambda \in H_0^1(\Gamma_f) \times \mathbb{R} \text{ such that:} \\ \\ \forall v \in H_0^1(\Gamma_f),\ \lambda m_s(w, v) = a_s(w, v), \\ \\ m_s(w, w) = 1. \end{array} \right. \tag{34}$$

The family of solutions $\{w_n\}$ is an Hilbert basis of the space $[\tilde{H}^{1/2}(\Gamma_f)]'$ which is ordered such that:

$$\lambda_1 \leq \lambda_2 \leq \ldots \leq \lambda_n \leq \lambda_{n+1} \leq \ldots$$

Furthermore the basis is also conjugate versus the bilinear form a_s. Let us denote by P the smallest integer such that $\lambda_P > 0$. Let us set:

$$\eta^n = \sum_{n \geq 1} \alpha_j^n w_j. \tag{35}$$

Hence from (32) one deduces that:

$$\begin{aligned} &\forall j \geq 1,\ \forall n \geq 1, \\ &|\frac{\alpha_j^{n+1}-\alpha_j^n}{\Delta t}|^2 + \frac{\lambda_j}{2}|\alpha_j^{n+1}|^2 = (\frac{\alpha_j^{n+1}-\alpha_j^n}{\Delta t})\,(\frac{\alpha_j^n-\alpha_j^{n-1}}{\Delta t}) + \frac{1}{2}\lambda_j|\alpha_j^n|^2. \end{aligned} \tag{36}$$

This implies the stability for any component α_j^n such that $j \geq P$. But for $j < P$ one only has from an induction argument (where the constant c depends

on initial conditions):

$$|\frac{\alpha_j^{n+1}-\alpha_j^n}{\Delta t}|^2 - |\lambda_j||\alpha_j^{n+1}|^2 \leq c. \tag{37}$$

Because this estimate is optimal (Schwarz's inequality) it proves that the solution η_j^n is instable. One can check it by considering the particular sequences which satisfies (37) and which tends to the infinity as soon as $\Delta t\sqrt{|\lambda_j|} < 2$:

$$\alpha_j^{n+1} = \frac{\alpha_j^n}{1-\Delta t\sqrt{|\lambda_j|}}. \tag{38}$$

But the numerical test performed on the progressive wave model are still more convincing. The simulation have performed with and without the surface laplacian but the result are quite identical (the results presented are obtained with this term). Furthermore the influence of the capillary is analyzed and one can see that the influence is fundamental, even for flow velocities U smaller than the first critical value U_c. The results have been plotted on figure 9 for $\sigma = 7,5\ 10^{-2}\ Nm^{-2}$ (with capillary) and $\sigma = 0$ (without capillary), $\varrho = 10^3\ Kg$. One can observe that as soon as the critical velocity (here $U_c = 0.161\ m/s$) is overtaken, the scheme is fully instable and much more than the physical solution. This transfer of energy is due to the gyroscopic coupling (because it is the only mean to do that) which extracts energy from the stable eigenmodes and delivers it onto the instable eigenmodes. For this reason one can claim that the scheme (33) should be avoided for the development of the instability. This result which is true for the linear model is also true for the non linear progressive wave model.

3.3.2 A more appropriate scheme of the instable wave model $U \geq U_c$.

Let us now consider another time step scheme for the wave equation by setting (let us again consider that the laplacian $\delta_s\tilde{\Phi}_0$ is neglected for the theoretical discussion) :

$$\left\{\begin{array}{l} \text{find } \eta^{n+1} \in V^h \text{ such that } \forall v \in V^h, \\ \\ m_s(\eta^{n+1}-2\eta^n+\eta^{n-1},v) + U\Delta t c_s(\eta^{n+1}-\eta^{n-1},v) \\ \\ \qquad\qquad + \dfrac{\Delta t^2}{2} a_s(\eta^{n+1}+\eta^{n-1},v) = F(v). \end{array}\right. \tag{39}$$

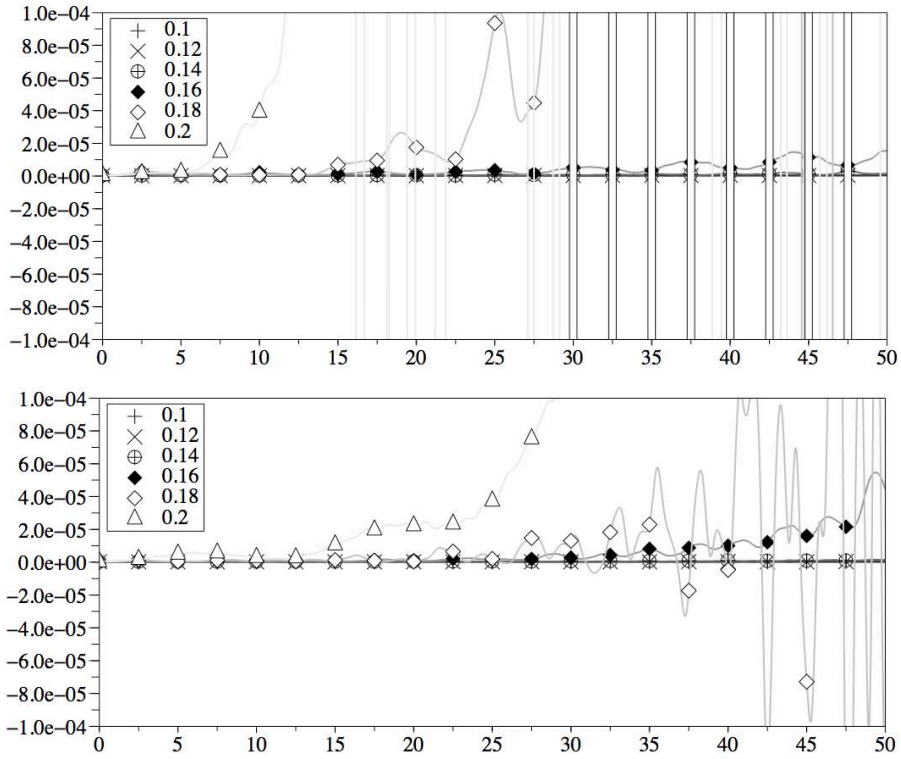

Figure 9: Instable time-evolution of the energy for the linear model for the scheme (31) and for several velocities ($U > U_c$ and $U < U_c$). Top for $\sigma = 0$ and bottom for $\sigma = 7,5\ 10^{-2}$.

Setting $v = \eta^{n+1} - \eta^{n-1}$ in this relation, one obtains (the gyroscopic term disappears because $\mathcal{C}_s$ is antisymmetrical):

$$\begin{aligned} m_s(\frac{\eta^{n+1}-\eta^n}{\Delta t}, \frac{\eta^{n+1}-\eta^n}{\Delta t}) + \frac{1}{2}a_s(\eta^{n+1}, \eta^{n+1}) \\ = m_s(\frac{\eta^n-\eta^{n-1}}{\Delta t}, \frac{\eta^n-\eta^{n-1}}{\Delta t}) + \frac{1}{2}a_s(\eta^{n-1}, \eta^{n-1}). \end{aligned} \tag{40}$$

In fact this quantity is an approximation of the energy $E(n)$ of the mechanical system (progressive waves) at time $t = n\Delta t$ is obtained as far as η^n and $\eta^{n\pm1}$ are close, because:

$$E(n) = \frac{1}{2}m_s(\frac{\eta^{n+1}-\eta^n}{\Delta t}, \frac{\eta^{n+1}-\eta^n}{\Delta t}) + \frac{1}{2}a_s(\eta^n, \eta^n). \tag{41}$$

The important point is that this expression is constant for the scheme (39). Hence it keeps the energy or at least a quantity which is equivalent to it. Therefore even for instable movement this scheme is better adapted. The numerical tests are plotted on figure 10. The values of the physical constants are the same as in the scheme (31). One can observe that the stabilities observed are close to the true physical solution as far as a capillary energy is kept. The justification is that only the instable eigenmodes generate instable approximate solutions.

3.4 Visualization of the surface wake

Let us consider in this section two simulations of the progressive water waves occuring at the free surface. The first case corresponds to a submarine moving forwards from the right to the left at a given velocity and quite close to the free surface (see figure 11). The second one concerns the influence of a rocky bottom (see figure 12). The geometry of the bottom is the one shown on figure 2. It is a superposition of several sinusoïdes. It is an artificial approximation of real pebble stone bottom. But it should be point out that a slight random perturbation of the pebbles stones on the bottom can induce a large variation on the shape of the instabilities as far as the wave lenghts are close to the one of the instabilities represented by the eigenvectors solution of (25). But this would be another study. One important point is that the instabilities on the surface of the water are localized (at the beginning) above the submarine and everywhere in the second case concerning the pebble stone bottom. Furthermore the pebble stone distribution has been chosen such that the wave lenght is different from the one of the eigenmodes of the pool in order to avoid artificial resonances. In both cases the movement is initiated by the digging effect η_0 due to the term $-\frac{\varrho}{2}|\nabla_s\Phi_0|^2$ at the right hand side of the wave equation (10).

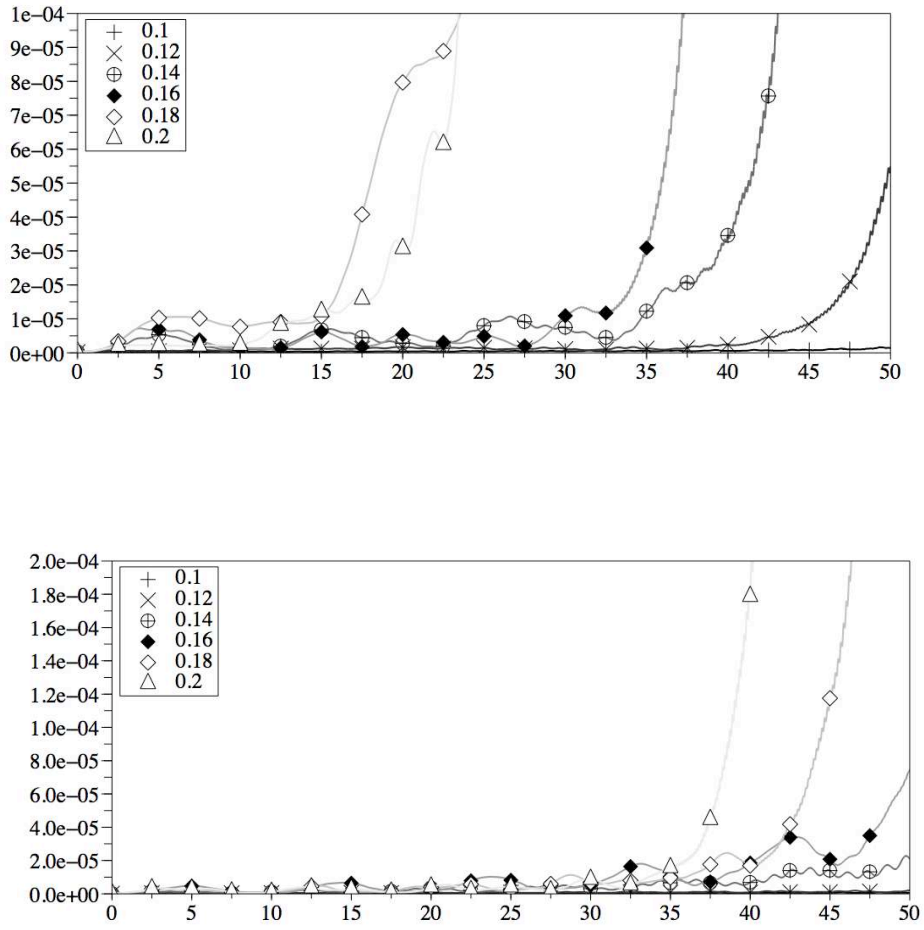

Figure 10: Instable time-evolution of the energy for the linear model for the scheme (39) for several velocities ($U > U_c$ and $U < U_c$): top without capillary, bottom with $\sigma = 7.510^{-2}$

3.4.1 The case of the submarine

One can observe that the surface becomes instable at the vertical of the submarine. Thus the instability is transfered everywhere on the surface. This is due to the fact that a Venturi effect appears between the surface of the water and the submarine. Therefore the velocity is locally larger and the surface is sucked downwards in a first step. Then a wave appears in the wake. This phenomenon is always true but it is much more amplified over the critical velocity. Because the spectral density is high around the first eigenvalue which is the square of the first critical velocity, the mechanism becomes more and more complex for larger velocities which imply several eigenvectors.

3.4.2 Visualization of the surface wave for the pebble stone bottom

Several velocities have been considered for the steady flow. The depth is fixed and the four first graphs correspond to a velocity smaller than the critical value obtained from the smallest eigenvalue of (25). The simulation is performed with the linear model and the shape of the bottom is represented on the last graph of these graphics. The two following correspond to instable velocities. One can observe on figure 12 that the progressive waves depend strongly on the value of this velocity compared to the first critical value. But because of the high spectral density several instable eigenvectors are concerned for instance if $U \geq 0.2m/s$. This is justified from figure 6. Hence the instable movement which is generalized on all the free surface is a very complex one.

3.4.3 The wake with a non-linear term

The two cases (submarine and pebble stone bottom) are discussed in this subsection. For $U \geq \sqrt{\lambda_1}$ the linearized model of the surface is instable. Simulations where the non-linear term:

$$\frac{\varrho}{2} \int_{\Gamma_f} [|\nabla_s \varphi|^2 + |\frac{\partial \eta}{\partial t} + U \nabla_s \tilde{\Phi}_0 . \nabla_s \eta|^2],$$

has been added to the equation (19). In the numerical computation this term is computed using backward time step difference in order to be explicit on the non linear term. One could object that there are other non-linear terms which have been omitted. Therefore the simulation given hereafter are only an indication of what can happen.

The submarine (non-linear) The visualization of the wake observed is plotted on figure 13 for the submarine. One can observe an amplification of the solution compared to the linear one, even when the the linearized model is stable.

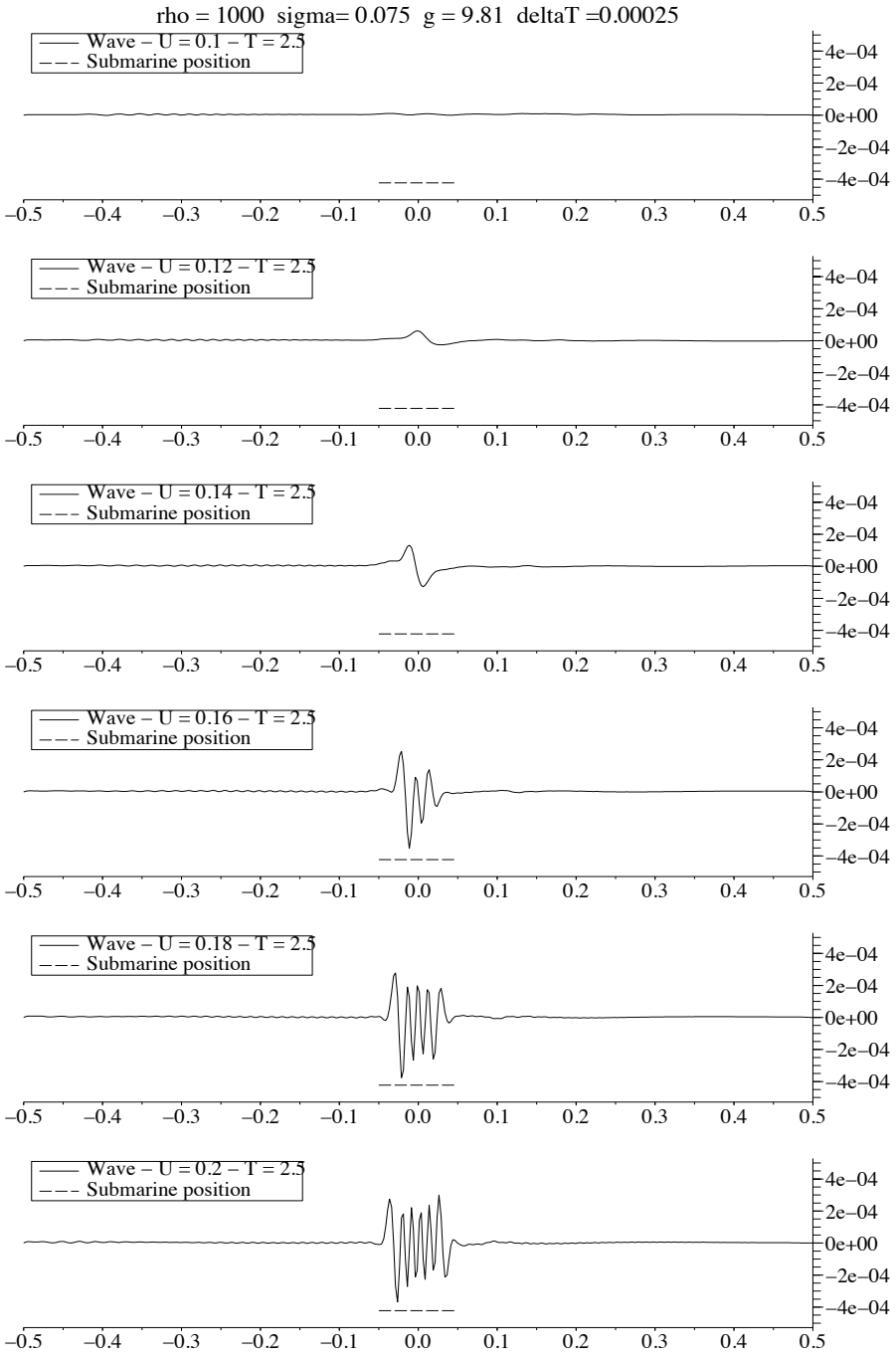

Figure 11: Wake above a submarine for different velocities of the steady flow: $0.1\ m/s \leq U \leq 0.2\ m/s$

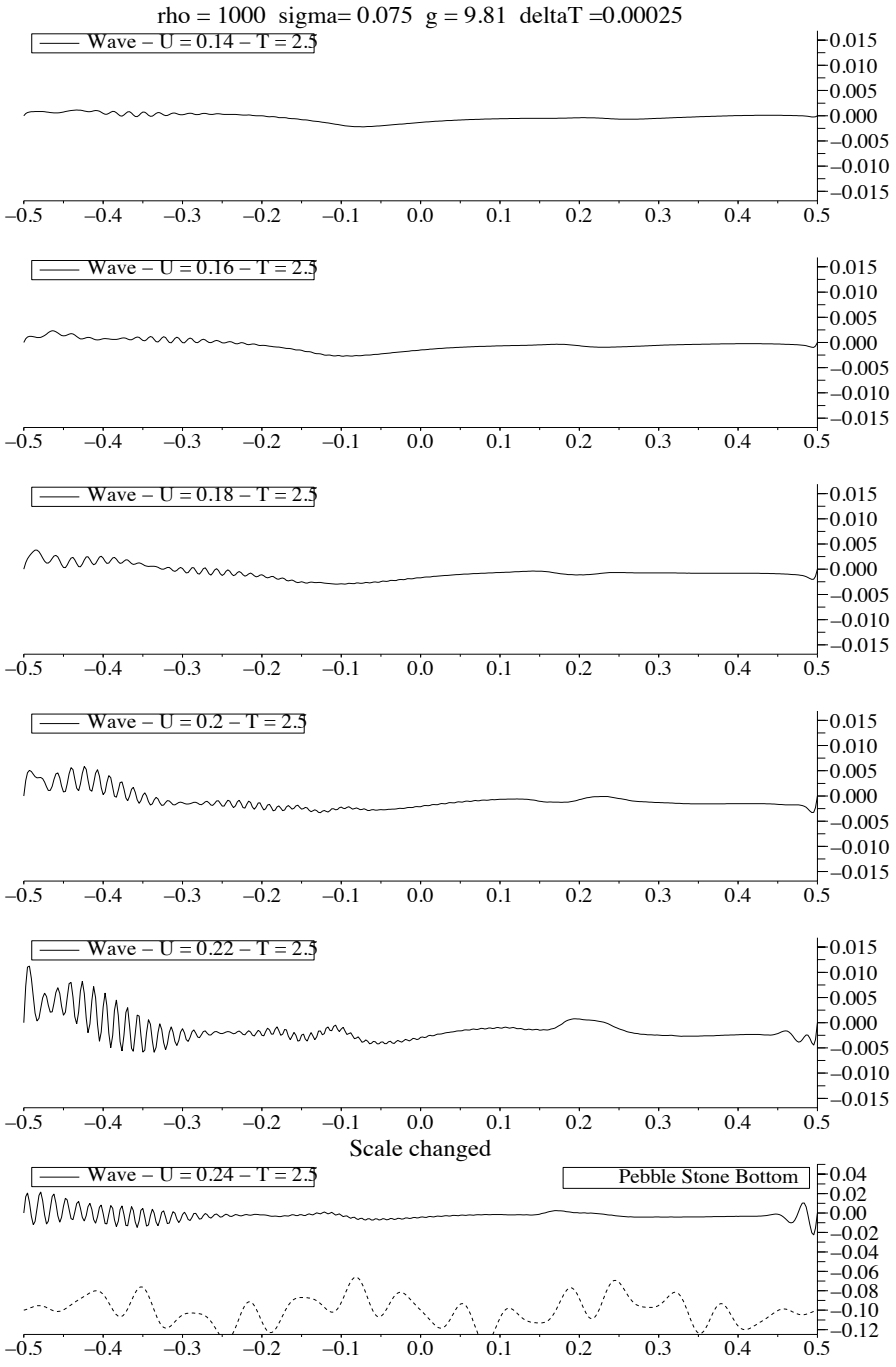

Figure 12: Progressive waves for a small depth: $0.14\ m/s \leq U \leq 0.24\ m/s$

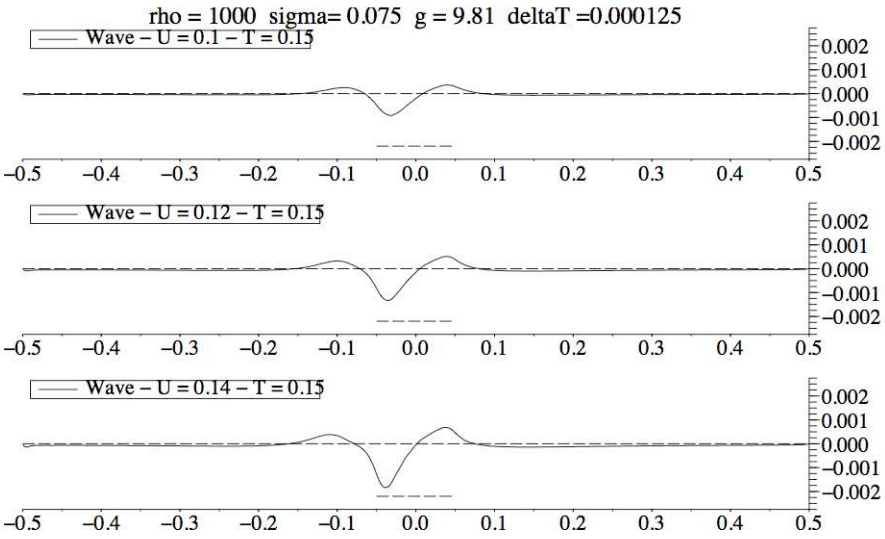

Figure 13: Non linear solution of the progressive wave model with a submarine for $U = 0.1m/s,\ 0.12m/s,\ 0.14m/s$.

The pebble stone bottom (non-linear) One point in the non linear case is that the instability seems to be more structured that in the linear case. There can be a reason. The non linear term that has been introduced (which is not complete) selects among the instabilities those which are non-linearly stable and those which are instable.

Concerning the non-linear analysis, the results published up to now mainly concern a simplified model in which there are no boundary condition and furthermore there is no submarine or pebble stone bottom. The first mathematical contribution is the paper by T. Brooke Benjamin and J. E. Feir [BEN 67] who detected the possibility of an instability on a water surface flow under the effect of a periodic paddle excitation at a given frequency. Most of the references (both theoretical and applied ones) [IOS 96], [DIKH 99], [CHA 07] concern a finite dimensional approximation and mainly without capillary. Furthermore the numerical tests are mostly restricted to case where one can use the integral representation for the velocity potential of the solution, which is not adapted to the geometry discussed here.

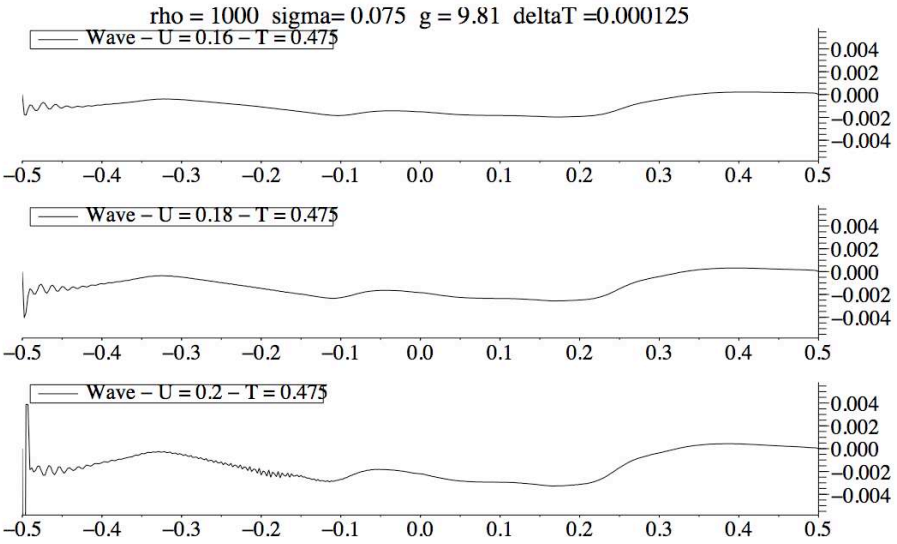

Figure 14: Non linear solution of the progressive wave model for several velocities $U = 0.16m/s,\ 0.18m/s,\ 0.2m/s$. The simulation concerns the pebble stone model.

4 Conclusion

In this paper a modification of the Neumann-Kelvin's wave model for the instable progressive wave is discussed from the numerical point of view. Let us underline the main points.

1 The role of the capillary is explained in mathematical framework for the physical equations for progressive waves. It is proved that the classical Neumann-Kelvin's model is fully instable and should be modified in order to be mechanically reliable.

2 It is shown that the best way to take the capillary into account is to use a formulation where the normal displacement η of the free surface appears as a main unknown variable. In particular cases one can eliminate the velocity potential φ making use of the added mass operator. This operator plays a basic role in the balance energy between the gravity and the capillary. On simple examples the first instability due to the velocity U occurs when the energy of the capillary reach the same level as the one of the gravity (see the example treated J. Lighthill [LIH 78]). But in more general cases, this critical velocity is characterized by an eigenvalue problem. As far as one has to consider a coupling of the sea with a ship, the formulation in η is more appropriate than

the one in φ. For instance the slamming between the shell of the ship and the surface of the water can be formulated with respect to η. Furthermore the mathematical model of progressive waves formulated in η -even if it is equivalent to the one in φ- has better properties for the numerical implementation.

There are other physical mechanisms which should be added to the progressive wave model. For instance the vortex have been eliminated in the potential model, but the viscosity should play a role on the damping of wave and the characterization of the critical velocity U_c. The compressibility of the water is certainly acceptable inside the water, but much less for the surface waves. The coupling with the atmosphere is a fundamental problem and it can change a lot the behaviour of the progressive waves, mainly if temperature gradient is meaningful.

Our goal was only to focus on the validity (in fact the non validity) of the Neumann-Kelvin's model) for which a modification is suggested in order to overcome classical difficulties mentioned in many scientific contributions.

References

[Aub 02] G. Aubert P. Kornprobst, *Mathematical Problems in Image Processing*, Applied mathematical sciences, **147**, Springer, Berlin, (2002).

[ADA 75] R. Adams, *Sobolev spaces,* Academic press, New York, (1975).

[KON 06] M. Borsuk and V. Kondratiev, *Elliptic Boundary Value Problems of Second Order in Piecewise Smooth Domains,* North Holland, Mathematical Library, Amsterdam, (2006).

[BEN 67] T. Brooke Benjamin and J. E. Feir, The desintegration of wave trains on deep water, Part 1 Theory. J. Fluid Mech., vol. **27**, pp. 417-430, (1967).

[BRE 83] H. Brezis, *Analyse Fonctionnelle,* edition Masson, Paris, (1983).

[CAM 02] E. F. Campana and A. Iafrati, Direct numerical simulation of surface tension dominated and non-dominated breaking waves, 24^{th} symposium on Naval hydrodynamics, Fukuoka Japan, July (2002).

[CHA 07] D. Chalikov, Numerical simulation of the Benjamin-Feir instability and its consequences, Physics of fluids, American Institute of Physics, **19**, 016602, (2007).

[CHEN 01] Xiao-bo Chen, On the singular and highly oscillatory properties of the Green function for ship motions, J. Fluid Mechs., vol. 445,pp. 77-91, (2001).

[CHEN 02] Xiao-bo Chen, Role of the surface tension in modelling ship waves, Proc. of the 17^{th} Inter. Workshop on water Waves and floating bodies, edited by R. C. Rayney and S. F. Lee, Peterhouse Cambridge, UK 14-17 april, pp. 25-28, (2002).

[DCF 08] Ph Destuynder, C. Fabre, A modelling of springing, whipping and slamming for ships, Communications on Pure and Applied Analysis, vol. 8, $n^0 1$, pp. 209-228, (2008).

[DCF 09] Ph. Destuynder, C. Fabre, A discussion on Neumann-Kelvin model for progressive water waves, Internal research report CNAM, (2009).

[DIKH 99] F. Dias and C. Kharif, Non-linear Capillary and capillary-gravity waves, Annu. Rev. Fluid Mech., **31**, pp. 301-346, (1999).

[DOU 95] Y. Doutreleau, Résonances pour le problème de Neumann-Kelvin tridimensionnel dans le cas d'un corps immergé, 5^{th} journées de l'hydrodynamique, Rouen, mars (1995).

[DUV 90] G. Duvaut, *Mécanique des milieux continus,* Dunod, Paris, (1990).

[GAZZ 05] Th. Gazzola, A. Korobkin, Sime Malenica and Yves-Marie Scolan, Three- dimensional Wagner problem using variational inequalities, in "Proceedings of the 20^{th} International Workshop on Water Waves and Floating Bodies," (2005).

[GAZ 07] Th. Gazzola, Modélisation du phénomène de tossage pour les bateaux, Thèse de l'Ecole Centrale de Paris, (2007).

[GRI 86] P. Grisvard, *Singularities In Boundary Value Problems,* Masson, Paris, (1992).

[TIM 85] A.J Hermans, G.C Hsiao and R. Timman, *Water waves and ship hydrodynamics*, Delft University Press, The Netherlands, (1985).

[HOL 04] D. S. Holloway, G. A. Thomas and M. R. Davis, Added mass of whipping modes for ships at high Froude number by a free surface boundary element method coupled with strip theory, ANZIAM J., **45** (2004), C831-C844.

[IOS 96] G. Ioss P. Kirrmann, Capillary Gravity Waves on the Free Surface of an Inviscid Fluid of Infinite Depth, Existence of Solitary Waves, Arch. Rational Mech. Anal. vol. 136, pp. 1-19, Springer-Verlag, (1996).

[KEL 87] Kelvin Lord (Sir Thomson), On the waves produced by a single input in water of any depth, or in a dispersive medium, In: *Proceedings of the Royal Society of London*, series A, vol. 42, pp. 80-85, (1887).

[LAL 71] L. Landau, E. Lipschitz, *Mécanique des fluides,* Editions de Moscou, (1971).

[LIH 78] J. Lighthill, *Waves in fluids,* Cambridge university press, (1978).

[LM 68] J. L. L. Lions and E. Magenes, *Problèmes aux limites non homogènes et applications, Tome 1,* Dunod, Paris, (1968).

[MRO 92] J. P. Morand and R. Ohayon, *Interactions fluides-structures,* RMA $n^0$23, Masson, Paris, 1992.

[NEC 67] J. Necas, *Les méthodes directes en théorie des équations elliptiques,* Masson, Paris, 1967.

[RATO 83] P. A. Raviart and J. M. Thomas, *Introduction à l'analyse numérique des équations aux dérivées partielles,* Masson, Paris, 1983.

[RIC 96] D. Richard and P. G. de Gennes, Capillary gravity waves caused by a moving disturbance wave resistance, J. Phys. Rev. E., vol. 53, pp. 3448-3455, (1996).

[STOE 92] C. Van der Stoep, 'A three dimensional method for the calculation of the unsteady ship wave pattern using a Neumann-Kelvin approach, Thesis university of technology of Delpht, February 6^{th} 1992.

[STO 57] J. J. Stoker, *Water waves*, Pure and applied mathematics, vol. IV, Interscience publishers, Inc., New York (1957).

[TIM 85] R. Timman, A.J. Hermans and G.C. Hsiao, *Water waves and ship hydrodynamics,* Delft university-press, the Netherlands, (1985).

[TRU 01] K. Trulsen and C. T. Stansberg, Spatial evolution of water surface waves: Numerical simulation and experiment of bichromatic waves, Proceedings of the eleventh international offshore and polar engineering conference, Stavanger, Norway, June 17-22, 2001.

[YAN 00] C. Yang, R. Lohner, F. Noblesse and Th. T. Huang, Calculation of ship sinkage and trim using unstructured grids, ECCOMAS 2000, Barcelona, 11-14 September, (2000).